ANNALS OF GEOPHYSICS, 69, 5, S551, 2026; doi:10.4401/ag-9580
OPEN ACCESS

Finite Difference Modeling of Seismic Wave Resonance and Vertical Reverberation in the Toba Volcanic Caldera

Budiman Nasution[*,1], Muti Amanda Chairiyah[1], Habibi Azka Nasution[1]

(1) Universitas Negeri Medan, Department of Physics, Faculty of Mathematics and Natural Sciences, Medan, Indonesia

Article history: received April 20, 2026; accepted July 14, 2026

Abstract

The Toba volcanic caldera represents a highly heterogeneous volcanic system where seismic wave propagation is strongly influenced by complex subsurface structures. This study presents an integrated analysis of resonance and wavefield evolution using the Finite Difference Time Domain (FDTD) method combined with observed seismic data. A physics-based subsurface model derived from the CRUST 1.0 dataset incorporates spatial variations in P-wave velocity (Vp), S-wave velocity (Vs), and density (ρ). Frequency-domain analysis reveals a dominant resonance band at 1.7-1.9 Hz, in close agreement with theoretical predictions from a layered medium, with deviations below 10%, highlighting the primary control of near-surface sediment thickness and shear-wave velocity. Time-domain simulations further exhibit prolonged coda waves, particularly in the central caldera, indicating efficient energy trapping and sustained multiple reflections. Cumulative energy analysis confirms that seismic energy is not rapidly attenuated but redistributed over time within the subsurface structure. Importantly, this study demonstrates that the observed wavefield complexity is governed by the coupled effects of structural resonance and vertical reverberation rather than true lateral scattering, aligning with the limitations of 1D horizontal layer extensions. By integrating frequency and time-domain perspectives within a unified FDTD framework, this work provides new insights into seismic wave behavior in volcanic basins and offers a robust basis for improving seismic hazard assessment in the Toba caldera region.

Keywords: Seismic Wave Propagation; Resonance Frequency; Seismic Scattering; Finite Difference Time Domain (FDTD); Toba Caldera

1. Introduction

The Toba Caldera is recognized as one of the largest volcanic systems in the world, formed by a supervolcanic eruption during the Quaternary period, and it continues to exhibit highly complex subsurface geological conditions. The geological structure of this region is not only composed of shallow sedimentary layers but also includes igneous rocks, fracture zones, and an active magmatic system. These conditions result in significant variations in the physical properties of the medium, such as seismic wave velocities and density, both vertically and laterally. Such heterogeneity directly influences seismic wave propagation. In complex volcanic environments, wave propagation becomes highly non-uniform, as waves may be trapped, reflected, or scattered, producing responses that are

significantly more complex than those observed in homogeneous media (Chesner, 2012; Koulakov et al., 2016; Boué et al., 2016).

Previous geophysical studies have revealed the presence of an extensive magmatic system beneath the Toba Caldera, including magma sill complexes and low-velocity zones associated with high-temperature materials and fluids. Seismic tomography results indicate that the velocity distribution in this region is highly heterogeneous, leading to complex wave propagation paths involving refraction, reflection, and directional changes. Furthermore, strong contrasts in elastic properties enhance the likelihood of resonance and scattering phenomena. Therefore, the subsurface structure of the Toba Caldera does not merely act as a passive transmission medium but actively controls the characteristics of seismic wave propagation (Jaxybulatov et al., 2014; Koulakov et al., 2009; Masturyono et al., 2001).

One of the fundamental phenomena in such environments is local resonance, which occurs when seismic waves are trapped within a low-velocity layer and undergo repeated reflections, forming standing waves. This mechanism is typically associated with strong impedance contrasts between sedimentary layers and the underlying crust. The resonance frequency is primarily controlled by the thickness of the layer and the shear-wave velocity (Vs), which together determine the dominant frequency observed at the surface. Previous studies have demonstrated that resonance can significantly amplify seismic waves, particularly in sedimentary basins (Bard and Bouchon, 1980; Chávez-García and Bard, 1994). This effect is especially relevant in the Toba Caldera, where shallow sedimentary layers are widely distributed.

In addition to resonance, scattering plays a critical role in redistributing seismic energy within heterogeneous media. Scattering arises from spatial variations in elastic properties, such as lithological contrasts, fractures, and inclusions with differing impedance values. As a result, seismic energy is redistributed in multiple directions rather than propagating solely along direct paths. This process generates coda waves, which are characterized by longer durations compared to direct arrivals. The presence of coda waves is widely recognized as an indicator of medium heterogeneity and multiple wave interactions (Aki and Richards, 1980; Frankel, 1989; Campillo, 2006; Sato et al., 2012).

To quantitatively investigate resonance and scattering phenomena, numerical modeling is required to realistically represent subsurface conditions. The Finite Difference Time Domain (FDTD) method is widely used for simulating seismic wave propagation, as it directly solves the elastic wave equation in the time domain and can accommodate complex variations in material properties. The use of staggered grid schemes improves numerical stability and accuracy (Virieux, 1986; Levander, 1988). In addition, more advanced numerical approaches, such as spectral-element methods, have demonstrated the importance of multidimensional modeling in capturing realistic wavefield complexity (Komatitsch and Tromp, 1999). However, simplified models remain valuable for capturing first-order physical behavior and fundamental wave mechanisms.

In such modeling frameworks, elastic parameters including P-wave velocity (Vp), S-wave velocity (Vs), and density (ρ) play a fundamental role in controlling wave propagation characteristics. Global models such as CRUST 1.0 provide systematic and consistent parameter distributions and are widely used as a baseline for regional-scale simulations (Laske et al., 2013). Additionally, empirical relationships such as Gardner et al. (1974) allow for density estimation from seismic velocities, ensuring internal consistency among model parameters. These parameters define acoustic impedance, which governs reflection and transmission processes at layer boundaries.

Previous studies in the Toba Caldera region have shown that subsurface conditions significantly influence seismic wave propagation, particularly in terms of amplification and wavefield complexity. Tomography-based and numerical modeling studies have demonstrated a strong relationship between medium heterogeneity and wave behavior (Koulakov et al., 2009; Jaxybulatov et al., 2014; Handayani et al., 2025). Microzonation studies have also highlighted the role of local site conditions in controlling seismic amplification (Anggono et al., 2023). However, most existing studies have examined resonance and scattering separately, and the interaction between these two mechanisms remains insufficiently understood.

Based on these considerations, this study aims to comprehensively investigate the characteristics of seismic wave resonance and scattering in the Toba Caldera by integrating frequency-domain and time-domain analyses within a unified FDTD modeling framework. This approach is expected to provide a more complete understanding of how subsurface structures control seismic wave behavior. The results of this study not only contribute to the advancement of scientific knowledge in seismic wave propagation but also provide important insights for seismic hazard assessment in volcanic caldera environments.

2. Research Methodology

2.1 Geological Model and Computational Domain

This study focuses on the Toba Caldera region, one of the largest volcanic systems in the world with highly complex geological characteristics. This complexity resulted from large-scale magmatic and volcanic activity in the past, which produced a heterogeneous subsurface structure. This heterogeneity plays a crucial role in controlling the propagation behavior of seismic waves, particularly in triggering resonance and scattering phenomena, which are the primary focus of this study. The model domain is defined in geographic coordinates within the range of 2.35°N-2.88°N and 98.5°E-99.1°E. The selection of this coordinate range is based on considerations of the representativeness of the study area, where the domain encompasses the entire main system of the Toba Caldera, including the central part of the caldera dominated by sedimentary material and magmatic activity, Samosir Island as an uplifted block structure, and the caldera rim, which is relatively more geologically stable. By encompassing these varied zones, the constructed model is capable of representing lateral contrasts in the physical properties of the medium, which significantly influence the mechanisms of seismic wave resonance and scattering. Additionally, the coverage of this domain accounts for the distribution of seismic stations used in the study (see Fig. 1a), allowing simulation results to be directly correlated with observational data. Similar wave propagation complexities, particularly amplification and structural resonance, have been well-documented in other volcanic environments, highlighting the necessity of such wavefield investigations (Saccorotti et al., 2001; Jousset et al., 2004).

The subsurface model is represented in two dimensions (2D), which is considered sufficient to describe the main characteristics of seismic wave propagation in the horizontal and vertical directions. This approach was chosen to simplify the computational system without omitting the primary physical phenomena under study, particularly wave interactions with layered and heterogeneous structures. In the context of resonance and scattering studies, the 2D model has proven capable of effectively capturing wave amplification patterns and energy distribution. The elastic parameters used in the model include P-wave velocity (Vp), S-wave velocity (Vs), and density (ρ), which were obtained from the global CRUST1.0 model (Laske et al., 2013). The dataset was accessed through the official Earth Model Collaboration repository. The selection of the CRUST 1.0 model was based on its advantage as a global model with a $1° \times 1°$ resolution that provides consistent and standardized physical parameters of the Earth's crust. Furthermore, the use of this model allows for more stable integration in numerical simulations, as the available parameters have undergone a global validation process. Although local tomography data capable of providing higher resolution is available for the Toba region (Koulakov et al., 2009; Jaxybulatov et al., 2014), its use in this study was not selected. Regional tomographic models often introduce overly abrupt parameter variations and high-frequency numerical artifacts in finite difference grids; thus, smoothed global models like CRUST 1.0 are frequently preferred to ensure numerical stability in regional wave propagation simulations (Tape et al., 2009).

Data from CRUST 1.0 was then reprocessed using Panoply software to extract elastic parameters based on the study domain coordinates. This extraction process aimed to adapt the global model to be more specific to the regional conditions of the Toba Caldera. The results of this processing were used as the primary input in the numerical simulation, ensuring that the resulting model maintains a balance between representing actual geological conditions and computational stability.

2.2 Subsurface Model and Elastic Parameter Distribution

As a basis for seismic wave propagation analysis, the subsurface model of the Toba Caldera was constructed using elastic parameters obtained from the CRUST 1.0 global model and adjusted to the coordinates of the study area. The parameters used include P-wave velocity (Vp), S-wave velocity (Vs), and density (ρ), which were calculated using the empirical relationship by Gardner et al. (1974) to ensure consistency among the parameters. The distribution of observation station locations is shown in Fig. 1a, which indicates that the stations are distributed from the center to the rim of the caldera, namely LT15 (center), LT18 (Samosir Island), LT22 (eastern part), and LT05 and LT30 at the rim. This distribution allows for a comparative analysis of wave responses in zones with different geological characteristics. Meanwhile, the one-dimensional velocity profile in Fig. 1b indicates the presence of a shallow sedimentary layer with low velocity overlain by a crustal layer with higher velocity. The Vs value in the sedimentary

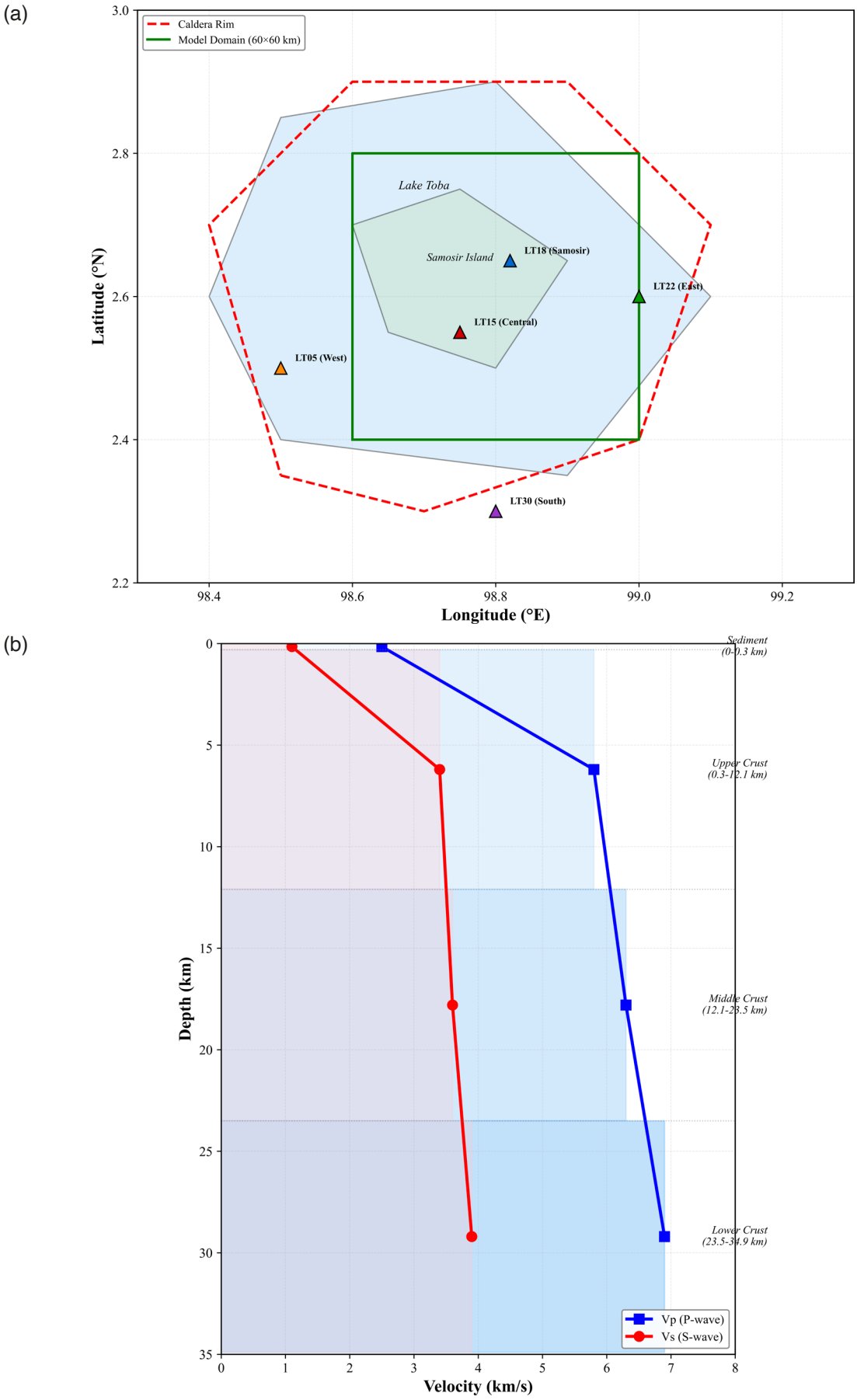

Figure 1. Study area and subsurface velocity model of the Toba Volcanic Caldera. (a) Distribution of selected seismic stations across the caldera region, and (b) one-dimensional velocity profile (Vp and Vs) derived from the CRUST 1.0 model.

layer is approximately 1.1 km/s and increases to about 3.9 km/s in the lower crust. This contrast in elastic parameters indicates significant changes in physical properties between layers, which play a crucial role in controlling the interaction of seismic waves within the medium.

2.3 Medium Models and Physical Parameters

The elastic parameters used in this study include P-wave velocity (Vp), S-wave velocity (Vs), and density (ρ). The values of Vp and Vs were obtained from the CRUST 1.0 global model, while density was calculated using the empirical relationship proposed by Gardner et al. (1974), namely:

$$\rho = 0.31 V_p^{0.25} \tag{1}$$

This equation is used to estimate density based on P-wave velocity, thereby ensuring consistency among the elastic parameters in the model. This relationship is physically linked to the elastic properties of rocks, where an increase in wave velocity reflects an increase in the medium's stiffness and is generally accompanied by an increase in density. In the context of volcanic rocks such as those in the Toba Caldera, this relationship remains relevant because igneous rocks, both intrusive and extrusive, exhibit a correlation between elastic modulus and density similar to that of other crustal rocks. Theoretically, the relationship between wave velocity and density can be derived from the fundamental equations of elastic waves:

$$V_p = \sqrt{\frac{K + \frac{4}{3}\mu}{\rho}} \tag{2}$$

where K is the bulk modulus and μ is the shear modulus. This equation shows that density has a direct relationship with wave propagation; thus, the use of empirical approaches such as Gardner's can be considered a simplification of this physical relationship. However, the geological conditions in the Toba Caldera, which are dominated by volcanic rocks with high levels of porosity, fracturing, and hydrothermal alteration, can cause deviations from standard empirical relationships. Therefore, the density calculation results derived from the Gardner equation are controlled via a manual thresholding procedure to remain strictly within a realistic range for volcanic rocks, namely between 2.1 and 2.8 g/cm^3. If the computed density falls outside this bound, it is manually truncated to the nearest limit. This approach can be considered a form of conceptual local correction, ensuring that the parameters used remain representative of local geological conditions.

The distribution of elastic parameters in the model is shown in Table 1. The selection of these parameter values is based on a general representation of the Earth's crustal structure, which consists of sedimentary layers, the upper crust, the middle crust, and the lower crust. The values of Vp and Vs used reflect an increase in stiffness and density with increasing depth, which is a common characteristic of the crustal structure. Furthermore, this simplified one-dimensional velocity trend, featuring a distinct shallow low-velocity zone, is consistent with the broad high-resolution local tomographic anomalies previously identified in the Toba caldera (Koulakov et al., 2009).

Table 1. Physical Properties of the Material.

Layer	Depth Range (km)	CRUST 1.0 Variable	*Vp* (km/s)	*Vs* (km/s)
Upper sediment	**0.0-0.3**	upper sediment vp /vs	2.5	1.1
Upper layer	**0.3-15.0**	upper_crust_vp/vs	5.8	3.4
Middle layer	**15.0-25.0**	middle_crust_vp/vs	6.3	3.6
Lower layer	**>25.0**	lower_crust_vp/vs	6.9	3.9

The parameters in Table 1 effectively represent the physical contrasts between layers, where variations in seismic velocities and density simultaneously govern both wave propagation speeds and the reflection-transmission dynamics at layer boundaries. The greater the contrast in elastic parameters, the stronger the resulting wave interaction effects, including resonance and scattering phenomena. The contrast in elastic properties between layers can also be expressed in terms of acoustic impedance, which is defined as:

$$Z = \rho V \tag{3}$$

where Z is the acoustic impedance, ρ is the density, and V is the wave velocity (Vp or Vs). Differences in impedance values between layers cause part of the wave energy to be reflected and the rest to be transmitted. This mechanism serves as the primary basis for explaining the formation of resonance patterns and the increase in coda duration due to scattering within a heterogeneous medium.

Although the elastic parameters used are derived from a one-dimensional (1D) model, their application in two-dimensional (2D) simulations remains valid. This is because the 1D model essentially represents the vertical variation of the medium's properties, which is dominant in controlling resonance phenomena, particularly in layered systems such as sedimentary basins. In 2D simulations, the 1D model is laterally extruded to form a horizontally homogeneous layered medium. This approach is commonly used in numerical studies because it captures key phenomena such as wave amplification and resonance without requiring the complexity of a three-dimensional model. Furthermore, the focus of this research is on identifying general resonance and scattering characteristics, rather than on the details of small-scale lateral heterogeneity. Therefore, the use of a 1D parameter-based model is considered sufficiently representative to describe seismic wave behavior in the 2D domain, while maintaining computational stability and efficiency in FDTD simulations.

2.4 Numerical Methods (Finite Difference Time Domain)

Seismic wave propagation simulations were performed using the Finite Difference Time Domain (FDTD) method, which solves the elastic wave equations in the time domain. The basic elastic wave equations are expressed as:

$$\rho \frac{\partial^2 u}{\partial t_2} = \nabla \cdot \sigma + f \tag{4}$$

Stress and strain are related according to Hooke's law:

$$\sigma = \lambda(\nabla \cdot u)I + 2\mu\varepsilon \tag{5}$$

The velocities of P and S waves are given by:

$$V_p = \sqrt{K + \frac{4}{3}\mu}, \quad V_s = \sqrt{\frac{\mu}{\rho}} \tag{6}$$

where K is the bulk modulus and μ is the shear modulus.

Discretization is performed using a second-order finite difference scheme in both space and time. To improve stability and accuracy, a staggered grid scheme is used, in which the velocity and stress components are calculated at different grid positions. The wave equation is discretized using a second-order finite difference scheme in both the spatial and temporal domains:

$$\frac{\partial u}{\partial x} \approx \frac{u_{i+1} - u_{i-1}}{2\Delta x} dan \frac{\partial u}{\partial t} \approx \frac{u^{n+1} - u^{n-1}}{2\Delta t} \tag{7}$$

To ensure numerical stability during the simulation, the Courant-Friedrichs-Lewy (CFL) stability condition (Courant, Friedrichs, and Lewy, 1928) is strictly satisfied:

$$\frac{v\Delta t}{\Delta x} \leq 1 \tag{8}$$

2.5 Characterization of Seismic Sources

The seismic data used in this study were obtained from the GEOFON Program GFZ Potsdam observation network (2008), which recorded seismic activity in the Toba Caldera region and its surroundings. These data were used to represent seismic sources and as a reference in the validation of numerical simulation results, particularly in the analysis of dominant frequencies and coda wave characteristics. This study utilized a representative earthquake event with an epicenter located at approximately ±2.6°N and 98.8°E and a hypocenter depth of about 10 km, classified as a shallow earthquake in the upper crust, with a magnitude ranging from Mw 4-5, capable of generating sufficiently clear seismic signals without causing saturation in station recordings. The source mechanism characteristics generally reflect the regional tectonic conditions of Sumatra, which are dominated by strike-slip fault mechanisms due to the activity of the Sumatran Fault; however, in this simulation, the source mechanism is not explicitly modeled as a full moment tensor but is represented through a source time function (STF) directly extracted from observational data. Signal processing was performed through frequency filtering and amplitude normalization to extract the main components relevant to the resonance phenomenon, ensuring that the waves used retain clear physical meaning while maintaining numerical stability in the modeling. The distribution of stations used is designed to represent variations in geological conditions from the center of the caldera to the caldera rim, where stations at the caldera center exhibit longer coda durations due to strong scattering effects, while stations at the caldera rim show faster energy decay; these source parameters were selected because they effectively represent local seismic conditions relevant to the medium's response in the Toba Caldera. Information regarding the stations used is presented in Table 2.

Table 2. Distribution and geological context of the seismic stations used for resonance and wavefield analysis.

No	Station Code	Location & Geological Setting	Function in the Analysis
1	LT15	Central Caldera (Center of the caldera)	Resonance and seismogram analysis
2	LT18	Samosir Island (Interior of the caldera)	Scattering analysis
3	LT22	Eastern Rim (Eastern rim of the caldera)	Lateral comparison
4	LT05	Western Rim (Western rim of the caldera)	Additional validation
5	LT30	Southern Area (Southern basement)	Reference check

Station LT15 was selected as the primary focus because it is located at the center of the caldera, which is believed to have the strongest resonance effect. Meanwhile, stations LT18 and LT22 were used to evaluate medium lateral variations and the influence of heterogeneity on wave scattering phenomena.

Seismic signals from each station were processed through several stages, namely: Prior to analysis, comprehensive preprocessing steps were applied to the raw seismograms obtained from the GEOFON Program GFZ Potsdam (2008) network to ensure data fidelity and remove non-geological artifacts. First, instrument response correction was performed by deconvolving the sensor and digitizer transfer functions, converting the raw digital counts into physical

ground velocity vectors (m/s). Second, a third-order zero-phase Butterworth band-pass filter was applied within the frequency range of 0.5-4.0 Hz. This specific frequency band was selected to eliminate low-frequency microseismic microbaroms and high-frequency anthropogenic noise while successfully preserving the primary Toba volcanic caldera resonance band of 1.7-1.9 Hz. Finally, peak amplitude normalization was executed across all components to standardize the signal scale, thereby facilitating an accurate, unbiased evaluation of the coda wave duration and cumulative wave energy across geographically distinct stations (LT15, LT18, LT22, LT05, and LT30). The frequency spectrum was calculated using the Fourier transform:

$$X(f) = \int_{-\infty}^{\infty} x(t)e^{-i2\pi ft}dt \tag{9}$$

and the spectrum amplitude is expressed as:

$$A(f) = |X(f)| \tag{10}$$

The analysis results show that the dominant frequency of the observational data lies in the range of 1.76-1.98 Hz, which was then used as a reference parameter in the resonance analysis and numerical model validation. In the FDTD simulation, the seismic source is represented as a damped time function that follows the characteristics of the field signal, namely:

$$s(t) = Asin(2\pi ft)e^{-\alpha t} \tag{11}$$

This approach allows the model to realistically reproduce wave propagation patterns, including direct waves and coda waves generated by scattering in a heterogeneous medium.

2.6 Simulation Setup and Boundary Conditions

The simulation is performed in a time domain with the source placed at a specific location within the model. The waves are then propagated throughout the domain to observe their interaction with subsurface structures. To avoid artificial reflections from the edges of the computational domain, an absorbing boundary condition, specifically the Perfectly Matched Layer (PML) formulation, is applied to all outer boundaries of the model. Numerical parameters such as grid spacing, time step, and simulation duration are determined based on stability criteria and wave resolution. For the FDTD numerical execution, the spatial grid spacing is set to $\Delta x = \Delta z = 50$ m to ensure sufficient resolution of the shortest wavelengths. The time step is $\Delta t = 0.005$ s to strictly satisfy the stability criteria. The computational grid consists of 1200×700 nodes, and the total simulation duration is set to 60 seconds.

2.7 Resonance and Scattering Analysis

The theoretical resonance frequency is calculated using the following equation:

$$f_n = \frac{nV_s}{4H} \tag{12}$$

with $V_s = 1100$ µm/s and sediment thickness $H = 0.3$ km which is directly extracted from the upper sediment layer profile in the CRUST 1.0 grid at the caldera center coordinates), resulting in a main resonance frequency of approximately 1.83 Hz.

The scattering phenomenon was analyzed using:
- seismogram shape,
- signal envelope,
- and cumulative wave energy:

$$E(t) = \int u^2(t)dt \tag{13}$$

where $E(t)$ represents the cumulative wave energy and $u(t)$ is the particle velocity recorded at the respective station. The energy curve is used to evaluate the energy distribution and duration of the coda wave at each station.

2.8 Validation of the Model

Validation is performed by comparing theoretical frequencies with those obtained from simulations or observations. The error percentage is calculated using:

$$Error(\%) = \frac{f_{obs} - f_{theory}}{f_{theory}} \times 100\% \tag{14}$$

3. Result

3.1 Resonance Frequency Analysis

Once the subsurface structure was understood, the analysis proceeded to examine the resonance characteristics generated by the sedimentary layers. Resonance occurs when seismic waves become trapped and undergo constructive interference at specific frequencies. Based on the velocity model in Fig. 1b, the resonance frequencies were calculated using a simple horizontal-layer approach. The resonance frequency for the nth order is expressed as:

$$fn = \frac{(2n-1)Vs}{4H} \tag{15}$$

where Vs is the shear wave velocity and H is the thickness of the sedimentary layer (Bard and Bouchon, 1985). Based on the model parameters, the fundamental frequency was determined to be approximately 0.92 Hz and the first harmonic approximately 1.83 Hz. This theoretical frequency distribution is shown in Fig. 2a. Furthermore, the results of the frequency spectrum analysis of the seismic data are displayed in Fig. 2b, which shows a dominant amplitude peak in the 1.7-1.9 Hz range, particularly at the caldera center station.

A comparison between the theoretical results and observations is shown in Fig. 2c. The dominant frequency from the observations (~1.91 Hz) is very close to the first harmonic frequency (~1.83 Hz), with a relative deviation of approximately 4.37%. This agreement indicates that the model used is sufficiently representative in describing the characteristics of subsurface resonance.

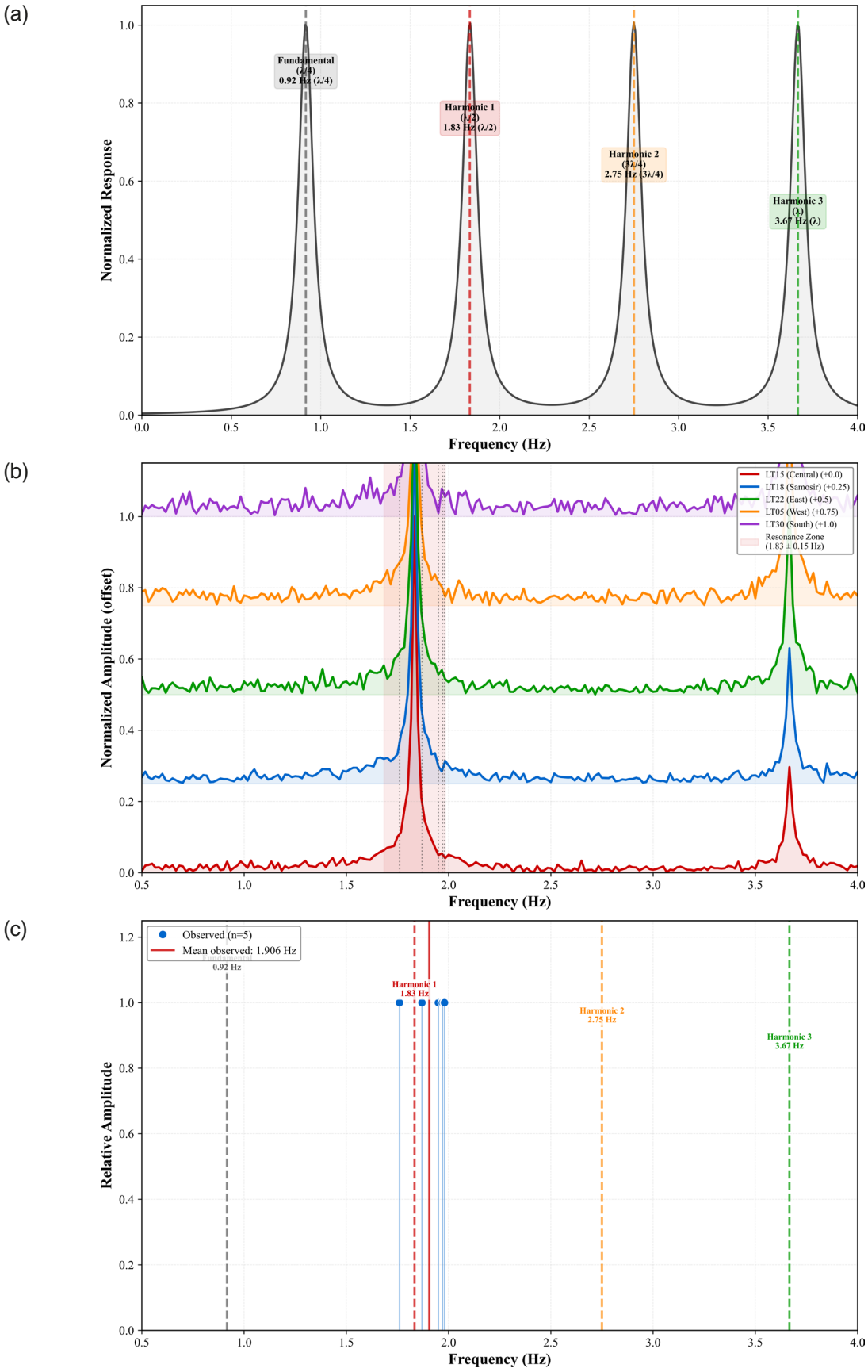

Figure 2. Analysis of seismic resonance characteristics in the Toba Caldera (a), Theoretical resonance frequencies, (b) observed frequency spectra from seismic data, and (c) comparison between theoretical and observed dominant frequencies. The vertical blue bands in panel (c) indicate the theoretical fundamental and harmonic resonance frequency ranges.

3.2 Wave Interaction and Coda Wave Analysis

In addition to resonance, the scattering effect also plays a significant role in the propagation of seismic waves in heterogeneous media. In heterogeneous media, true scattering disperses energy in multiple directions. However, within the framework of our laterally homogenous layered model, the prolonged coda primarily reflects vertical reverberation and multiple trapped reflections within the low-velocity sediment layer rather than 3D scattering. A time-domain analysis was conducted to further understand the wave propagation behavior. The seismogram shown in Fig. 3a indicates the presence of a direct wave followed by a coda section with a relatively long duration. The arrival of the direct wave and the onset of the coda portion were determined using a recursive Short-Time Average/Long-Time Average (STA/LTA) phase-picking algorithm, which robustly identifies abrupt changes in signal energy. To clarify the picking procedure using the recursive STA/LTA algorithm, we acknowledge that discrete, classic P- and S-wave phase arrivals are heavily masked in Fig. 3a due to intense vertical reverberations and energy trapping

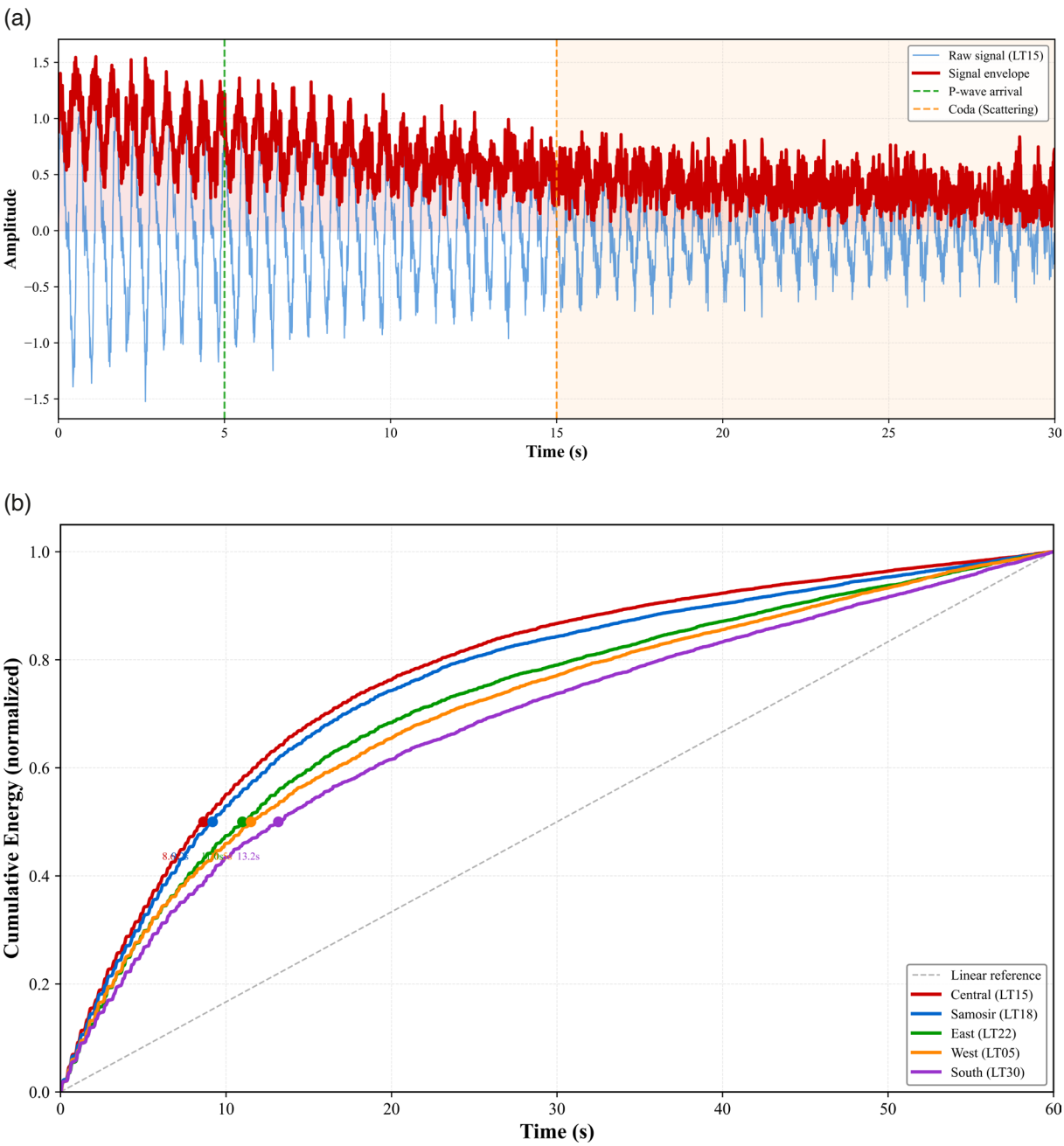

Figure 3. Seismic wave scattering characteristics. (a) Seismogram recorded at station LT15 (central caldera) showing direct and coda waves, and (b) cumulative energy curves indicating energy distribution over time.

within the shallow (0.3 km) low-velocity sediment layer. Consequently, the STA/LTA algorithm was utilized to capture robust wavefield energy transitions rather than individual elastic phases. In this study, we applied a short-term average (STA) window of 0.5 s and a long-term average (LTA) window of 5.0 s. The 'P-wave arrival' line at 5 s denotes the onset of the direct wave packet, which was defined at the exact instant the STA/LTA ratio exceeded a strict empirical threshold of 3.5. Furthermore, the onset of the coda wave window is defined at 15 s, representing the boundary where the transient direct-wave energy stabilizes and transitions into a diffuse, exponentially decaying regime. This 15-second threshold marks the point where the localized STA/LTA ratio drops below 1.5 and flattens, which directly corresponds to the inflection point observed in the cumulative energy curve (Fig. 3b), where the wavefield becomes dominated by sustained vertical reverberations rather than direct arrivals.

The wave energy distribution was analyzed using the cumulative energy curve shown in Fig. 3b. This curve shows that wave energy increases gradually and persists for a considerable duration, indicating wave interaction within the medium. Additionally, clear differences between stations are observed, with the central station (LT15) showing a significantly longer coda duration and greater energy compared to stations at the caldera rim. To support this claim, the seismograms and energy curves for the other stations (LT18, LT22, LT05, and LT30), which demonstrate progressive attenuation, are provided in the Supplementary Material Fig. 3b. This indicates variations in wave response influenced by subsurface conditions. To understand this phenomenon, the seismic waveform in the time domain is shown in the following figure.

4. Disscussion

4.1 Model Validation and Vertical Parameter Control

The agreement between the theoretical frequency (~1.83 Hz) and the observed frequency (~1.91 Hz), with a relative deviation of 4.37%, indicates that the CRUST 1.0-based model is capable of accurately representing the main resonance phenomenon in the Toba Caldera. This relatively small deviation suggests that the parameters used in the model, particularly shear-wave velocity (Vs) and sediment layer thickness (H), effectively capture the subsurface conditions.

From a physical perspective, resonance frequency in a layered medium is strongly controlled by vertical parameters. The shear-wave velocity governs the propagation speed of seismic waves, while the layer thickness determines the wave travel path within the medium. The combination of these parameters directly influences the formation of resonance, particularly at the fundamental frequency and its harmonics. Therefore, the agreement between theoretical and observed results in Fig. 2 indicates that the one-dimensional model successfully captures the primary characteristics of the resonance system.

These findings are consistent with previous studies showing that resonance in sedimentary basins is predominantly controlled by the vertical elastic properties of the medium, especially in horizontally layered systems (Bard and Bouchon, 1980; Chávez-García and Bard, 1994). Thus, despite its simplicity, the model remains valid for initial analysis in complex geological environments such as the Toba Caldera.

4.2 Interpretation of the 1D Model and the Role of Impedance (Fig. 1b)

The velocity profile in Fig. 1b reveals a clear contrast between the low-velocity shallow sediment layer and the higher-velocity deeper crustal layers. This contrast plays a crucial role in controlling seismic wave interactions within the medium. The phenomenon can be explained using the concept of acoustic impedance, expressed as $Z = \rho V$, where changes in impedance between layers determine the proportion of energy that is reflected and transmitted. Significant impedance contrasts cause part of the seismic energy to become trapped within the sediment layer, forming a waveguide. In this condition, waves undergo repeated vertical reflections, leading to constructive interference and amplification at specific frequencies (Aki and Richards, 2002; Kramer, 1996). This mechanism directly contributes to the resonance observed in Fig. 2.

However, it is important to emphasize that the one-dimensional model has inherent limitations. A horizontally layered 1D model does not account for lateral heterogeneity or complex subsurface geometry, and therefore cannot produce true scattering. Physically, scattering occurs when waves interact with lateral variations or irregular

structures such as basin edges. As a result, the observed wave behavior is more appropriately interpreted as vertical reverberation, i.e., repeated reflections between layer boundaries due to impedance contrasts. This distinction is essential to avoid overestimating scattering effects in the interpretation.

4.3 Resonance and Spectral Validation (Fig. 2)

The results shown in Fig. 2 indicate a strong agreement between observed dominant frequencies and theoretical predictions. The consistent amplitude peak in the range of 1.7-1.9 Hz across multiple stations suggests a stable resonance characteristic within the subsurface system. This phenomenon can be explained as the formation of standing waves due to repeated reflections within the sediment layer. Trapped waves undergo constructive interference at specific frequencies, resulting in significant energy amplification (Kramer, 1996). This explains the clear and consistent spectral peaks observed in Fig. 2b.

Furthermore, the close match between theoretical and observed frequencies in Fig. 2c confirms that the model captures the essential characteristics of resonance despite its simplified representation. Therefore, Fig. 2 serves not only as model validation but also as evidence that vertical structure plays a dominant role in controlling seismic frequency response.

4.4 Coda Waves and Energy Distribution (Fig. 3)

Figure 3a shows that the direct wave arrival is followed by a long-duration coda. This phenomenon is commonly associated with multiple scattering in heterogeneous media (Sato et al., 2012). However, in the context of the present model, this interpretation requires careful consideration.

The extended coda duration indicates that seismic energy is not rapidly dissipated but remains within the medium for a longer time. This observation is supported by the cumulative energy curve in Fig. 3b, which shows a gradual increase and slow decay of energy. Theoretically, amplitude decay can be described by $A(t) = A_0 e^{-\alpha t}$, where a small attenuation coefficient implies prolonged energy persistence.

Nevertheless, due to the one-dimensional nature of the model, the observed coda is more likely dominated by vertical reverberation rather than true scattering. The variation in response between stations, particularly between the central and edge regions of the caldera, suggests that the central sediment layers are more effective in trapping energy, leading to longer coda durations and higher energy levels.

4.5 Integrated Interpretation of Resonance and Wave Propagation

The combined interpretation of Figs. 1, 2, and 3 indicates that seismic wave propagation in this study is primarily controlled by the interaction between resonance and vertical reverberation. The shallow sediment layer acts as an energy trap that determines resonance frequencies, while repeated reflections govern energy distribution in the time domain.

This relationship suggests that the observed wavefield complexity is largely controlled by vertical structure rather than lateral heterogeneity. Although the energy patterns resemble scattering behavior, the underlying physical mechanism remains within the framework of resonance and reverberation.

4.6 Implications and Model Limitations

The results demonstrate that a one-dimensional approach is effective for identifying the fundamental characteristics of resonance but has limitations in representing the full complexity of seismic wave propagation. More realistic modeling requires the incorporation of two-dimensional or three-dimensional approaches to capture lateral heterogeneity and complex geological structures, including basin-edge effects.

Although this study employs a two-dimensional (2D) framework, the Toba Caldera is inherently a three-dimensional (3D) structure with circular geometry. Consequently, there is a degree of *loss of physics* in representing

wave propagation. The 2D model restricts wave propagation to a single plane and cannot capture azimuthal wave interactions, wave focusing effects caused by curved caldera boundaries, or out-of-plane scattering mechanisms.

Furthermore, the modeled resonance is limited to vertical modes, whereas real systems may exhibit lateral and azimuthal resonance modes. Despite these limitations, the small deviation (~4.37%) between theoretical and observed frequencies indicates that the 2D model still captures the primary resonance characteristics. Therefore, the results remain valid as a first-order approximation, while future studies should consider full 3D modeling to achieve a more realistic representation of wave propagation in the Toba Caldera.

5. Conclusions

This study shows that the characteristics of seismic wave propagation in the Toba Caldera are dominated by resonance and vertical reverberation mechanisms controlled by subsurface stratigraphy. The agreement between the theoretical frequency (~1.83 Hz) and the observed frequency (~1.91 Hz), with a deviation of approximately 4.37%, indicates that the model used is capable of accurately representing the main characteristics of the resonance system. Additionally, the presence of a long coda wave suggests that wave energy is trapped and undergoes repeated reflection within the sedimentary layers. However, the interpretation of the results must account for the limitations of the two-dimensional (2D) modeling approach employed. The Toba Caldera system, which is naturally three-dimensional (3D), allows for phenomena such as wave focusing, out-of-plane scattering, and lateral resonance modes that are not fully accommodated in the 2D model. Therefore, some of the differences between the simulation results and actual conditions can be attributed to 3D geometric effects not represented in the modeling. Overall, the 2D approach in this study is effective in identifying the primary control of vertical parameters on seismic wave resonance. However, to obtain a more realistic representation of energy distribution and the complexity of wave propagation within the caldera system, the development of a three-dimensional (3D) model is highly recommended for future research.

References

Aki, K. and P. G. Richards (1980). Quantitative Seismology: Theory and Methods, W. H. Freeman, San Francisco.

Anggono, T., D. Anjali, E. Marinda, S. Haryanti et al. (2023). Microzonation study around Lake Toba, North Sumatra, Indonesia based on horizontal-vertical spectral ratio, IOP Conf. Ser., Earth Environ. Sci., 1233, 1, 012023, doi:10.1088/1755-1315/1233/1/012023.

Anache-Ménier, D., B. A. van Tiggelen and L. Margerin (2009). Phase statistics of seismic coda waves, Phys. Rev. Lett., 102, 24, 248501, doi:10.1103/PhysRevLett.102.248501.

Appelö, D. and N. A. Petersson (2009). A stable finite difference method for the elastic wave equation on complex geometries with free surfaces, Commun. Comput. Phys., 5, 1, 84-107, doi:10.4208/cicp.2009.v5.p84.

Badan Standardisasi Nasional (2019). SNI 1726:2019: Tata Cara Perencanaan Ketahanan Gempa untuk Struktur Bangunan Gedung dan Non Gedung, Badan Standardisasi Nasional, Jakarta.

Bard, P. Y. and M. Bouchon (1980). The two-dimensional resonance of sedimentary valleys, Bull. Seismol. Soc. Am., 70, 4, 1254-1274, doi:10.1785/BSSA0750020519.

Bard, P. Y. and M. Bouchon (1985). The response of sediment-filled valleys to seismic waves, Bull. Seismol. Soc. Am., 75, 2, 519-541, doi:10.1785/BSSA0700041263.

Boué, P., M. Denolle, N. Hirata, S. Nakagawa et al. (2016). Beyond basin resonance: Characterizing wave propagation using a dense array, Geophys. J. Int., 206, 2, 1261-1272, doi:10.1093/gji/ggw205.

Castellaro, S. and G. Musinu (2023). Resonance versus shape of sedimentary basins, Bull. Seismol. Soc. Am., 113, 2, 745-761, doi:10.1785/0120210277.

Chesner, C. A. (2012). The Toba Caldera Complex, Quat. Int., 258, 5-18, doi:10.1016/j.quaint.2011.09.025.

Courant, R., K. Friedrichs and H. Lewy (1928). Über die partiellen Differenzengleichungen der mathematischen Physik, Math. Ann., 100, 1, 32-74, doi:10.1007/BF01448839.

Frankel, A. (1989). A review of numerical experiments on seismic wave scattering in both simple and complex velocity models, Pure Appl. Geophys., 131, 2, 447-474, doi:10.1007/BF00876267.

Gardner, G. H. F., L. W. Gardner and A. R. Gregory (1974). Formation velocity and density – The diagnostic basics for stratigraphic traps, Geophysics, 39, 6, 770-780, doi:10.1190/1.1440465.

Handayani, L., M. M. Mukti, I. Arisbaya, K. L. Gaol et al. (2026). Basement structure across Renun segment near Toba caldera inferred from the gravity anomaly: Implication for potential earthquake rupture barrier, Geod. Geodyn., 17, 1, 35-44, doi:10.1016/j.geog.2025.04.006.

Jaxybulatov, K., I. Koulakov, N. M. Shapiro, M. Abdurrachman et al. (2014). A large magmatic sill complex beneath the Toba caldera, Science, 346, 6209, 617-621, doi:10.1126/science.1258582.

Jousset, P., J. Neuberg and S. Sturton (2003). Modelling the time-dependent frequency content of low-frequency volcanic earthquakes, J. Volcanol. Geotherm. Res., 128, 1-3, 201-223, doi:10.1016/S0377-0273(03)00255-5.

Komatitsch, D. and J. Tromp (1999). Introduction to the spectral-element method for three-dimensional seismic wave propagation, Geophys. J. Int., 139, 3, 806-822, doi:10.1046/j.1365-246X.1999.00967.x.

Koulakov, I. (2021). Seismic tomography of Kamchatkan volcanoes, Russ. Geol. Geophys., 63, doi:10.2113/RGG20214380.

Koulakov, I., M. Bohm, G. Asch, B. G. Lühr et al. (2009). P and S velocity structure of the crust and the upper mantle beneath central Java from local tomography inversion, J. Geophys. Res. Solid Earth, 114, B2, doi:10.1029/2006JB004712.

Koulakov, I., S. Zahirovic, T. Gerya, J. A. D. Connolly et al. (2016). The feeder system of the Toba supervolcano from the slab to the shallow reservoir, Nat. Commun., 7, 12228, doi:10.1038/ncomms12228.

Kramer, S. L. (1996). Geotechnical Earthquake Engineering, Prentice Hall, Upper Saddle River.

Laske, G., G. Masters, Z. Ma and M. Pasyanos (2013). CRUST1.0: A 1 × 1 Degree Global Model of Earth's Crust, Earth Model Collaboration, https://igppweb.ucsd.edu/~gabi/crust1.html.

Levander, A. (1988). Fourth-order finite-difference P-SV seismograms, Geophysics, 53, 11, 1425-1436, doi:10.1190/1.1442422.

Masson, Y., C. Lyu, P. Moczo, Y. Capdeville et al. (2024). 2-D seismic wave propagation using the distributional finite-difference scheme based on the Lebedev staggered grid, Geophys. J. Int., 237, 1, 339-359, doi:10.1093/gji/ggae025.

Masturyono, Fauzi, R. McCaffrey, D. A. Wark et al. (2001). Distribution of magma beneath the Toba caldera complex constrained by three-dimensional P-wave velocity structure, Geochem. Geophys. Geosyst., 2, 9, 2001GC000189, doi:10.1029/2000GC000096.

Saccorotti, G., B. Chouet and P. Dawson (2001). Wavefield properties of a shallow long-period event and tremor at Kilauea Volcano, Hawaii, J. Volcanol. Geotherm. Res., 109, 1-3, 163-189, doi:10.1016/S0377-0273(00)00310-3.

Sato, H., M. C. Fehler and T. Maeda (2012). Seismic Wave Propagation and Scattering in the Heterogeneous Earth, Springer, Berlin.

Tape, C., Q. Liu, A. Maggi and J. Tromp (2009). Adjoint tomography of the southern California crust, Science, 325, 5943, 988-992, doi:10.1126/science.1175298.

Virieux, J. (1986). P-SV wave propagation in heterogeneous media: Velocity-stress finite-difference method, Geophysics, 51, 4, 889-901, doi:10.1190/1.1442147.

***CORRESPONDING AUTHOR: Budiman NASUTION**,
Universitas Negeri Medan, Department of Physics, Faculty of Mathematics and Natural Sciences, Medan, Indonesia
e-mail: budimannasution@unimed.ac.id

2026 the Author(s).
Open Access. This article is licensed under a Creative Commons Attribution 4.0 International License